J Physiol 595.21 (2017) pp 6719–6733

The Journal of Physiology

Subunit-dependent oxidative stress sensitivity of LRRC8 volume-regulated anion channels

Antonella Gradogna, Paola Gavazzo, Anna Boccaccio and Michael Pusch

Istituto di Biofisica, Consiglio Nazionale delle Ricerche, Via De Marini 6, I-16149 Genova, Italy

Key points

- Swelling-activated anion currents are modulated by oxidative conditions, but it is unknown if oxidation acts directly on the LRRC8 channel-forming proteins or on regulatory factors.
- We found that LRRC8A–LRRC8E heteromeric channels are dramatically activated by oxidation of intracellular cysteines, whereas LRRC8A–LRRC8C and LRRC8A–LRRC8D heteromers are inhibited by oxidation.
- Volume-regulated anion currents in Jurkat T lymphocytes were inhibited by oxidation, in agreement with a low expression of the LRRC8E subunit in these cells.
- Our results show that LRRC8 channel proteins are directly modulated by oxidation in a subunit-specific manner.

Abstract The volume-regulated anion channel (VRAC) is formed by heteromers of LRRC8 proteins containing the essential LRRC8A subunit and at least one among the LRRC8B–E subunits. Reactive oxygen species (ROS) play physiological and pathophysiological roles and VRAC channels are highly ROS sensitive. However, it is unclear if ROS act directly on the channels or on molecules involved in the activation pathway. We used fluorescently tagged LRRC8 proteins that yield large constitutive currents to test direct effects of oxidation. We found that 8A/8E heteromers are dramatically potentiated (more than 10-fold) by oxidation of intracellular cysteine residues by chloramine-T or *tert*-butyl hydroperoxide. Oxidation was, however, not necessary for hypotonicity-induced activation. In contrast, 8A/8C and 8A/8D heteromers were strongly inhibited by oxidation. Endogenous VRAC currents in Jurkat T lymphocytes were similarly inhibited by oxidation, in agreement with the finding that LRRC8C and LRRC8D subunits were more abundantly expressed than LRRC8E in Jurkat cells. Our results show that LRRC8 channels are directly modulated by oxidation in a subunit-dependent manner.

(Received 18 June 2017; accepted after revision 16 August 2017; first published online 25 August 2017)

Corresponding author M. Pusch: Istituto di Biofisica, Consiglio Nazionale delle Ricerche, Via De Marini 6, I-16149 Genova, Italy. Email: michael.pusch@ge.ibf.cnr.it

Abbreviations CBX, carbenoxolone; chl-T, chloramine T; DTT, dithiothreitol; LRRC8, leucine rich repeat-containing protein 8; MMTS, *S*-methyl methanethiosulfonate; MTS, methanethiosulfonate; MTSES, 2-sulfonatoethyl methanethiosulfonate; MTSET, 2-(trimethylammonium)ethyl methanethiosulfonate; ROS, reactive oxygen species; TBHP, *tert*-butyl hydroperoxide; VRAC, volume-regulated anion channel.

Introduction

Cell volume regulation is an essential function for virtually all cells. In mammals volume regulation is physiologically important for proliferation, migration, signalling and apoptosis (Nilius *et al.* 1997; Schwab *et al.* 2012). The ubiquitously expressed volume-regulated anion channel (VRAC) mediates swelling-activated Cl^- currents in practically all cell types studied (Nilius *et al.* 1997). Activation of VRAC underlies the process of regulatory volume decrease, mediated by an efflux of KCl from the cells followed by water efflux. In addition to chloride, VRAC is also permeable to small organic molecules

DOI: 10.1113/JP274795

including taurine and excitatory amino acids, and even ATP (Okada *et al.* 2009; Gaitán-Peñas *et al.* 2016; Jentsch, 2016; Lutter *et al.* 2017). VRAC is also linked to the cell cycle and to proliferation. Cell shrinkage due to VRAC activation is essential for apoptosis, in a process called apoptotic volume decrease.

Until recently the gene(s) encoding VRAC were unknown, such that the physiological roles of VRAC could not be studied using molecular techniques. Only in 2014 two studies showed that the leucine rich repeat-containing protein 8A (LRRC8A) is an essential component of VRAC (Qiu *et al.* 2014; Voss *et al.* 2014), and four closely related homologues (LRRC8B to -E) are complementary VRAC subunits (Voss *et al.* 2014). VRAC channels are heteromers composed of at least one LRRC8A subunit and one member of the LRRC8B–E group (Voss *et al.* 2014; Gaitán-Peñas *et al.* 2016). LRRC8 proteins consist of ∼800 amino acids with a molecular mass of ∼95 kD. They are characterized by four transmembrane segments and contain up to 17 leucine-rich repeats (LRRs) in their cytoplasmic C-terminus (Abascal & Zardoya, 2012). LRRs are found in different proteins and are thought to participate in protein–protein interactions.

It is well established that VRAC activity is dependent on reactive oxygen species (ROS) (Browe & Baumgarten, 2004; Shimizu *et al.* 2004; Varela *et al.* 2004). In general VRAC activation is associated with an increase in ROS. ROS are implicated in a large variety of physiological and pathophysiological situations in all tissues. In tumours ROS are believed to be involved in proliferation of cancer cells. However, the role of ROS in cancer is not yet fully understood. For example, antioxidants can increase melanoma metastasis in mice (Le Gal *et al.* 2015) and distant metastasis induced in mice by human melanoma cells showed increased ROS (Piskounova *et al.* 2015). In addition to a pathological role in cancer, excessive ROS levels have been associated with ageing, but the evidence for this is still ambiguous (Lopez-Otin *et al.* 2013). Physiologically, ROS signalling plays an important role in the immune system (Muralidharan & Mandrekar, 2013). For example, neutrophils can eliminate pathogens by production of superoxide and other free oxygen radicals in phagosomes (DeCoursey, 2003).

Interestingly, T lymphocytes were among the first cells in which VRAC currents have been identified (Cahalan & Lewis, 1988; Lewis *et al.* 1993). Furthermore, *Lrrc8a* knockout mice exhibit defective development and function of T cells and increased thymocyte apoptosis (Kumar *et al.* 2014), suggesting an important role of VRAC for lymphocytes. However, the hypomorphic *ébouriffé* (*ebo*) mouse line that lacks the terminal 15 leucine-rich repeats in the LRRC8A subunit had no defect in T cell development or function (Platt *et al.* 2017). Also neutrophils from *ebo* mice retained phagocytic activity and had normal-sized vacuoles (Behe *et al.* 2017).

Given the broad physiological and pathophysiological relevance of the ROS sensitivity of VRAC it is important to decipher the molecular mechanisms underlying this regulation. However, a principal problem in studying the mechanisms of ROS sensitivity of VRAC channels is that it is difficult to distinguish direct effects of oxidizing conditions on the channel protein from indirect effects on other cellular components involved in the activation machineries. Here, we took advantage of our recent discovery that LRRC8 proteins can be conveniently expressed in *Xenopus* oocytes and that the addition of fluorescent proteins to their C-terminus leads to the expression of large constitutive currents (Gaitán-Peñas *et al.* 2016) to study the dependence of LRRC8 heteromers on oxidizing and reducing conditions.

We found that LRRC8 heteromeric channels are strongly regulated by oxidation. Surprisingly, LRRC8A/8E heteromers are dramatically potentiated by oxidation, whereas LRRC8A/8C and LRRC8A/8D heteromers are blocked. In the Jurkat T lymphocyte cell line, VRAC currents are inhibited by oxidation, in agreement with the hypothesis that currents are mostly carried by non-inactivating LRRC8A/8C channels, as also confirmed by RT-PCR which highlights a conspicuous expression of the LRRC8C gene.

Methods

Animals and ethical approval

Oocytes were obtained from *Xenopus laevis* frogs purchased from Harlan Laboratories (Udine, Italy) or directly purchased from Ecocyte Bioscience (Castrop-Rauxel, Germany). Oocytes were harvested from frogs that had been anaesthetized by tricaine (ethyl 3-aminobenzoate methanesulfonate salt, Sigma-Aldrich, Milan, Italy). After surgery, frogs were allowed to recover from anaesthesia and suitable aftercare was given. All animal protocols conformed to the European Community Guidelines on Animal Care and Experimentation and were approved by the Ethics Committee for Animal Experimentation of the Biophysics Institute.

Molecular biology and oocyte expression

All constructs used for heterologous expression have been described in detail (Gaitán-Peñas *et al.* 2016). Briefly, we used human *LRRC8A–E* cloned in the pCSDest vector. We used WT constructs as well as constructs in which Venus fluorescent protein (VFP) or mCherry was fused to the C-terminus. For expression in *Xenopus* oocytes, after linearization by *Not*I of the plasmids, cRNA of human LRRC8 proteins was transcribed using the mMessage mMachine SP6 kit (Thermo Fischer, Waltham, USA). Oocytes were defolliculated by a 1 h treatment with collagenase type I A (Sigma-Aldrich). Fifty nanolitres

cRNA, containing normally 12 ng of each subunit, was injected with a microinjector (Drummond, Broomall, USA, Nanoject II). Oocytes were incubated at 18°C in a solution containing (in mM): 90 NaCl, 2 KCl, 1 $MgCl_2$, 1 $CaCl_2$, 10 HEPES (pH 7.5).

Electrophysiology (voltage clamp)

One to three days after injection, voltage clamp measurements were performed using the custom acquisition program GePulse (available at http://users.ge.ibf.cnr.it/pusch/programs-mik.htm) and a Turbo-Tec-05X amplifier (npi electronics, Tamm, Germany). The standard extracellular solution contained (in mM): 100 NaCl, 2 KCl, 1.8 $CaCl_2$, 1 $MgCl_2$ and 10 HEPES (pH 7.3, osmolarity: 215 mosmol l^{-1}). Hypotonic solution contained (in mM): 48 NaCl, 2 KCl, 1.8 $CaCl_2$, 1 $MgCl_2$ and 10 HEPES (pH 7.3, osmolarity: 120 mosmol l^{-1}). Oxidizing and reducing reagents were freshly added at the desired concentration of 0.1–2 mM (chloramine-T), 0.25–1 mM (*tert*-butyl hydroperoxide (TBHP)) and 1 mM (*S*-methyl methanethiosulfonate (MMTS), 2-sulfonatoethyl methanethiosulfonate (MTSES), 2-(trimethylammonium)ethyl methanethiosulfonate (MTSET)) or 10 mM (dithiothreitol (DTT)). For MTSES and MTSET 100 mM stock solutions in distilled water were prepared and kept on ice for not longer than 2 h. Solutions were applied by continuous perfusion (solution exchange time <10 s). Carbenoxolone (CBX) was dissolved in the recording solution at 100 μM.

The voltage and time dependence of currents were assayed with a voltage-clamp pulse protocol consisting of a prepulse to −100 mV for 200 ms, followed by voltages ranging from −100 to 60 mV with 20 mV increments for 3000 ms. Pulses ended with a tail to −70 mV for 500 ms. Holding potential was −30 mV.

To assay the effects of oxidizing and reducing agents, a 200 ms pulse to 60 mV was applied every 5 s and currents were averaged over the pulse period and plotted as a function of time. In all figures, capacitive transients were blanked for clarity. For currents larger than ∼10 μA, series resistance was measured and compensated offline as follows. In current clamp a current pulse of 2 μA size was delivered and the initial fast rise in potential, ΔV, was attributed to the voltage-drop across the series resistance, $R_s = \Delta V/2\ \mu$A. For the voltage clamp protocols, the effective command voltage, V_{eff}, was then adjusted offline according to the calculated series resistance error by $V_{eff} = V_{command} - I \times R_s$, where I is the measured current. The current response at 60 mV was then corrected assuming a linear current–voltage relationship and the measured reversal potential.

All chemicals were purchased from Sigma-Aldrich except MTSES and MTSET, which were from Biotium (Fremont, California, USA).

Electrophysiology of Jurkat cells

Jurkat cells were kept in RPMI-1640 medium (Sigma-Aldrich) and were split every 3–4 days. For patch-clamp electrophysiology, a few microlitres of cells were transferred to a recording dish containing the recording extracellular solution. To activate VRAC with a hypertonic intracellular solution, patch pipettes of 2–4 MΩ resistance were filled with a solution containing (in mM) 160 caesium glutamate, 0.1 $CaCl_2$, 2 $MgCl_2$, 1.1 EGTA, 4 Na_2ATP, 10 HEPES, 50 sucrose (pH 7.2, ∼394 mosmol l^{-1}) as described in Lepple-Wienhues *et al.* (1998) and the extracellular solution contained 145 NaCl, 5 KCl, 2 $CaCl_2$, 1 $MgCl_2$, 10 HEPES, 10 glucose (pH 7.4, ∼315 mosmol l^{-1}). For activation of VRAC by extracellular hypotonicity, patch pipettes were filled with a solution containing (in mM) 160 caesium glutamate, 0.1 $CaCl_2$, 2 $MgCl_2$, 1.1 EGTA, 4 Na_2ATP, 10 HEPES (pH 7.2, ∼330 mosmol l^{-1}) and the extracellular solution contained (mM): 100 NaCl, 5 KCl, 2 $CaCl_2$, 1 $MgCl_2$, 10 HEPES, 10 glucose, 90 mannitol (pH 7.4, ∼315 mosmol l^{-1}). Cells were activated by a hypotonic solution lacking mannitol (∼212 mosmol l^{-1}). Chloramine-T (500 μM) was freshly added to the respective extracellular solutions. Activation was monitored by application of steps of 50 ms pulses to −100, −50, 0, 50 and 100 mV every 5 s from a holding potential of −50 mV (see Fig. 9). These steps allowed to verify the absence of a significant leak conductance because the expected reversal potential is ∼−50 mV and VRAC currents are strongly outwardly rectifying under the ionic conditions used (Lepple-Wienhues *et al.* 1998).

Statistical analyses

All data are reported as mean values ± standard error of the mean. Statistical significance was determined using Student's paired *t* test or one-sample *t* test, or ANOVA, as appropriate (Igor Pro, Wavemetrics, Lake Oswego, OR, USA). When a statistically significant difference was determined with ANOVA, a *post hoc* Tukey's test was used to evaluate which data groups showed significant differences. *P*-values < 0.05 were considered significant.

Real time qPCR

Jurkat cells (1.5×10^6) grown in suspension were collected by centrifugation and washed in phosphate-buffered saline (PBS). Total RNA was extracted using the Aurum Total RNA Mini Kit (Bio-Rad, Hercules, CA, USA) according to manufacturer's instructions. RNA concentration and purity were determined by measuring absorbance at 260 and 280 nm with a spectrophotometer. Two micrograms of total RNA were retrotranscribed to cDNA with RNAse H+ MMLV reverse transcriptase, including both

Table 1. Primers used in real-time qPCR

Gene	Amplicon length (bp)	Forward	Reverse
LRRC8A	109	ACAACAACCTGACCTTCCTC	GCACTGGAAGAGCTCCG
LRRC8B	143	TCTTTCGGGCTGTGTTCTCC	GCAATGAAGGCAGGAGGTCT
LRRC8C	142	AGCAGTTGCCAGTACCACTC	GAGGGCTCGCTCATAACACA
LRRC8D	136	CCCGATGCTGTCTTTGACCT	CAACTTTTGCAGGGCAGTGG
LRRC8E	146	ATCCCCCATGCAGTGTTCAG	ACGTAGGCGATCTGGTTGTG
ACTB	139	CTGGAACGGTGAAGGTGACA	AAGGGACTTCCTGTAACAAT

oligo(dT) and random primers in a 20 μl reaction (iScript Advanced cDNA Synthesis Kit for RT-qPCR, Bio-Rad). To determine the expression of LRRC8A–E subunits, cDNA was amplified in quantitative real-time PCR reaction using Sybr Green dye (SsoAdvanced Universal SYBR Green Supermix, Bio-Rad) and the Bio-Rad CFX Connect Instrument. The reaction conditions consisted of a polymerase activation/DNA denaturation step (3 min at 95°C), followed by 39 two-step cycles, each composed of a 10 s denaturation step at 95°C and a 40 s annealing/elongation step at 57°C. Actin (*ACTB*) was used as an internal control. No template control (NTC), no primer control (NPC), no reverse transcription control (NAC), consisting of a reaction without reverse transcriptase, were included in the qPCR reactions to exclude genomic DNA contamination and the presence of primer dimers. In order to check reaction specificity, a melting curve was generated after the amplification step. The sequences of the primers specific for LRRC8A–E subunits are listed in Table 1. In order to estimate PCR efficiency (E), standard curves were created for each LRRC8 subunit, using as template the plasmids containing the cDNAs of LRRC8 subunits (8A/8E). The concentration of each plasmid was initially determined with a spectrophotometer and then qPCR was performed on 1:10 serial dilutions of the templates, covering a range between 10^7 and 10^2 molecules. The plots of C_q (threshold cycle) *versus* the logarithm of the number of starting molecules were constructed for each target and fit with a straight line. The efficiency (E) of the reaction was estimated assuming an efficiency of 100% for a 1:10 serial dilution in case of a negative slope of $\log_{10}(0.5) \sim -3.3$.

Results

Activation of LRRC8A–VFP/8E–mCherry channels by oxidation

Recently we established *Xenopus* oocytes as an efficient system to study functional properties of VRAC channels formed by LRRC8 proteins (Gaitán-Peñas *et al.* 2016). Here, we used this system to investigate effects of oxidizing and reducing agents. In particular, we exploited the finding that the addition of fluorescent tags to the C-terminus of LRRC8 subunits induces large currents even in the absence of hypotonic stimulation (Gaitán-Peñas *et al.* 2016). We started with the LRRC8A–VFP/8E–mCherry subunit combination (for short 8A-VFP/8E-mCh), which yielded the largest currents (Gaitán-Peñas *et al.* 2016). Bath application of 1 mM of the oxidizing agent chloramine-T in isotonic conditions induced a dramatic current increase of 10- to 15-fold of 8A-VFP/8E-mCh-mediated currents recorded at a test potential of 60 mV from a holding potential of −30 mV (Fig. 1*A* and *F*). Currents were almost completely blocked upon application of the VRAC inhibitor CBX (100 μM; Fig. 1*A*). The current increase started after a delay of 20–30 s suggesting that chloramine-T had to enter the oocyte in order to exert its effect, as confirmed by more detailed studies (see below). The effect of the oxidizing reagent was not reversible upon washout of chloramine-T and only partially reversible upon application of the reducing agent DTT at 10 mM (less than 50% recovery, data not shown). The chloramine-T effect was dose-dependent: 0.1 mM was ineffective, while 2 mM did not result in higher currents compared to 1 mM (Fig. 1*B* and *F*).

Also application of the highly membrane-permeant oxidizing agent *tert*-butyl hydroperoxide (TBHP, 1 mM) led to a dramatic increase of 8A-VFP/8E-mCh-mediated currents in isotonic solution (Fig. 1*C* and *F*). Again, the onset of the current increase occurred after a significant delay following the application of TBHP suggesting an intracellular action of the oxidizing reagent. The minimal concentration at which we observed an effect was 0.5 mM, while 0.25 mM TBHP was almost ineffective within 5 min (Fig. 1*D*). The effect of TBHP developed at least 3 times more slowly than chloramine-T, preventing a proper quantification of the effect at lower concentrations. In contrast to chloramine-T, the TBHP effect was almost fully reversible upon application of 10 mM DTT (data not shown). However, as DTT is membrane permeant, this result does not provide information on the location of the residue(s) implicated in the activating oxidation reaction.

Applying 10 mM DTT without prior activation by oxidation had no effect on 8A-VFP/8E-mCh (Fig. 1*E* and *F*), suggesting that the constitutive currents exhibited by

these channels are not caused by an intrinsic oxidation process that can be reversed by DTT.

Importantly, application of chloramine-T or TBHP at 1 mM to uninjected oocyte did not induce significant currents within 5–10 min (Fig. 2). This finding, together with the observed block by CBX of the oxidation-induced currents in 8A-VFP/8E-mCh-expressing oocytes, strongly suggests that the oxidation-induced currents are mediated by the exogenously expressed 8A-VFP/8E-mCh heteromeric channels.

Interdependence of hypotonic stimulation and oxidation effects on LRRC8A–VFP/8E–mCherry channels

We asked if the activation of 8A-VFP/8E-mCh channels by oxidation mimics the 'regular' stimulation by hypo-osmotic conditions. To avoid series-resistance problems, for these experiments, we used oocytes with a small initial current. As seen in Fig. 3*A* application of chloramine-T after hypotonic activation of 8A-VFP/8E-mCh led to a large increase of the currents, suggesting that the two activating signals are additive. We next tested if the oxidation/reduction effects are artificially introduced by the C-terminal tags or if the same mechanisms are present in WT, i.e. untagged constructs. In isotonic conditions 8A/8E exhibited currents that were difficult to distinguish from background (Gaitán-Peñas *et al.* 2016; Fig. 3*B*). Nevertheless, addition of chloramine-T to 8A/8E-expressing oocytes activated a small but significant current with typical time and voltage dependence of 8A/8E channels (Fig. 3*B* and *D*), probably reflecting a minimal constitutive activity of 8A/8E without hypotonic stimulation. In this respect,

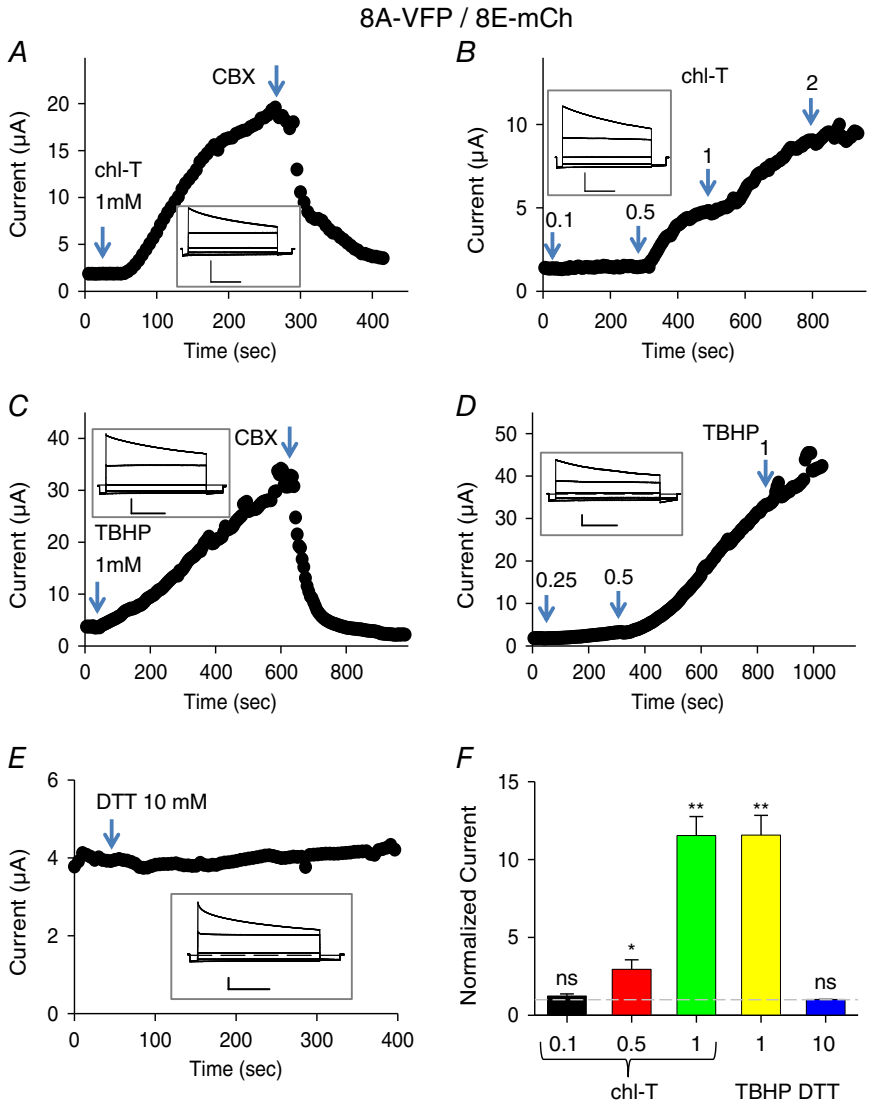

Figure 1. Activation of 8A-VFP/8E-mCh by oxidation
A–E, typical experiments illustrating the effect of application of chloramine-T (*A* and *B*), TBHP (*C* and *D*) or DTT to oocytes co-expressing 8A-VFP and 8E-mCh. The concentration is indicated in the figure. Time course of current recorded with a test pulse at +60 mV from a holding potential of −30 mV. Arrowhead indicates time of application of 100 μM CBX blocker. The inset shows the typical VRAC currents in response to an *I–V* protocol stimulation from −100 to +60 mV every 40 mV. Horizontal scale bars, 1 s; vertical scale bars, 1 μA (*A*, *C* and *E*), 2 μA (*B*) and 0.5 μA (*D*). *F*, average current response to the indicated stimuli, normalized to the initial current. Dashed line indicates basal current level (one-sample *t* test with respect to control value 1, 0.1 mM chloramine-T (chl-T), $P = 0.19$, $n = 4$; 0.5 mM chl-T, $P = 0.048$*, $n = 4$; 1 mM chl-T, $P = 0.00001$**, $n = 10$; 1 mM TBHP, $P = 0.00016$**, $n = 7$; 10 mM DTT, $P = 0.14$, $n = 3$; error bars indicate SEM). Please note the different time and current scales in the various panels. [Colour figure can be viewed at wileyonlinelibrary.com]

it is important to recall that we did not observe a chloramine-T effect (at 1 mM) on uninjected oocytes (Fig. 2). Hypotonicity significantly activated 8A/8E channels (Gaitán-Peñas *et al.* 2016; Fig. 3*C*). Importantly, applying chloramine-T (in a hypotonic solution) after the hypotonic activation led to a dramatic current increase (Fig. 3*C* and *D*) similar to that seen in 8A-VFP/8E-mCh (Fig. 1*A* and *F*).

Inhibition of LRRC8A–VFP/8C–mCherry and LRRC8A–VFP/8D–mCherry channels by oxidation

We next tested the oxidizing and reducing agents on 8A-VFP/8C-mCh and on 8A-VFP/8D-mCh heteromeric channels. Surprisingly, the constitutive currents of both combinations were inhibited by chloramine-T (Figs 4*A* and *D*, and 5*A* and *D*). In contrast TBHP had no significant effect on 8A-VFP/8C-mCh- (Fig. 4*B* and *D*) and on

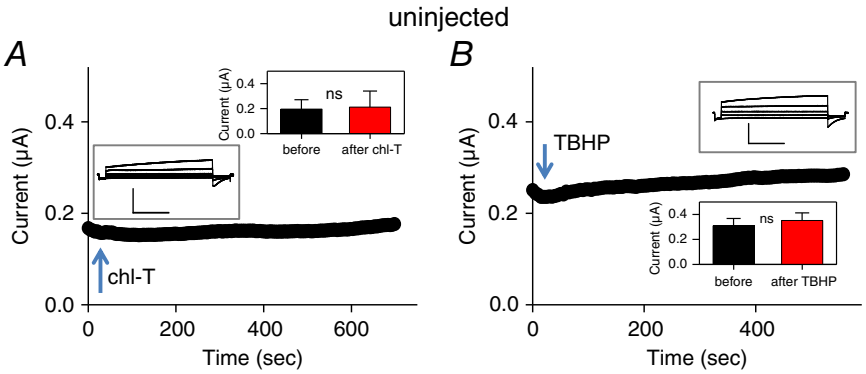

Figure 2. Application of oxidizing agents to uninjected oocytes
Experiments performed as in Fig. 1, illustrating the effect of application of 1 mM chloramine-T (*A*) or TBHP (*B*) from uninjected oocytes. The inset shows the typical endogenous currents in response to an *I–V* protocol stimulation from −100 to +60 mV every 40 mV. Current data values recorded at +60 mV before and after oxidizing reagent application are shown in the insets (paired *t* test for chl-T, $P = 0.64$, $n = 5$; for TBHP, $P = 0.095$, $n = 6$). Horizontal scale bars, 1 s; vertical scale bars, 0.5 μA. [Colour figure can be viewed at wileyonlinelibrary.com]

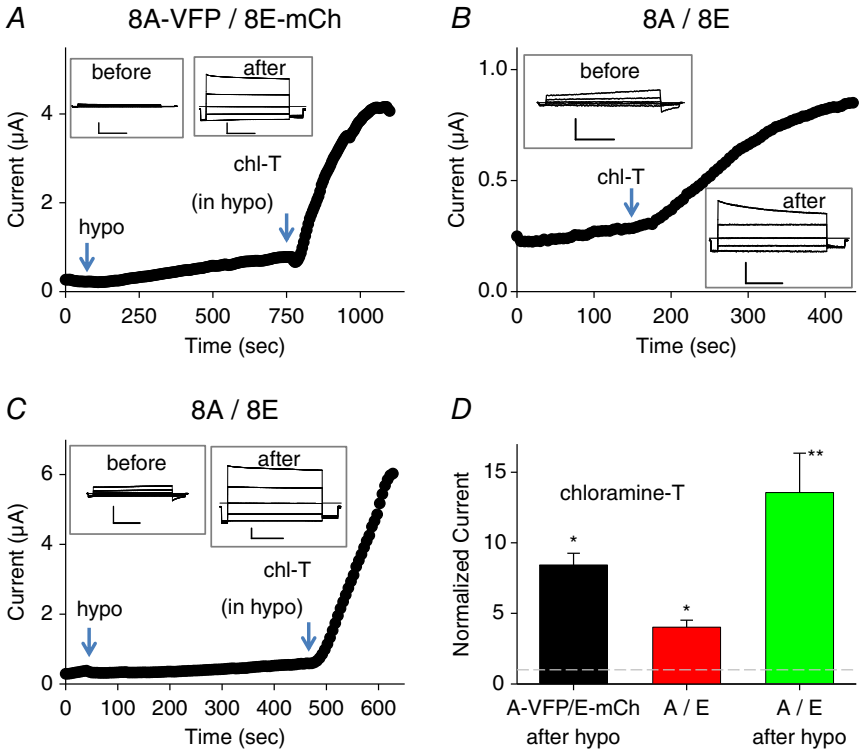

Figure 3. Effect of chloramine-T on hypotonicity activated 8A-VFP/8E-mCh and on WT 8A/8E
A, typical experiment illustrating the effect of application of 1 mM chloramine-T after hypotonic activation of an 8A-VFP/8E-mCh-expressing oocyte. The inset shows traces before hypotonic activation. *B* and *C*, typical experiments illustrating the effect of application of 1 mM chloramine-T on a WT 8A/8E-expressing oocyte without prior hypotonic stimulation (*B*) or after hypotonic stimulation (*C*). The insets show responses to an *I–V* stimulation before the hypotonic stimulus and after chloramine T application. Horizontal scale bars, 1 s; vertical scale bars, 1.5 μA (*A*), 0.5 μA (*B*), 0.5 μA (*C*, before) and 2 μA (*C*, after). *D*, average response to the indicated stimuli, normalized to the current before chloramine-T application (one-sample *t* test with respect to control value 1, 8A-VFP/8E-mCh in hypotonic bath, $P = 0.06$, $n = 3$; 8A/8E $P = 0.02$*, $n = 4$; 8A/8E in hypotonic bath, $P = 0.009$**, $n = 4$; error bars indicate SEM). Note the different time and current scales in the various panels. [Colour figure can be viewed at wileyonlinelibrary.com]

8A-VFP/8D-mCh- (Fig. 5*B* and *D*) mediated currents. Currents of both subunit combinations were significantly increased by DTT (Figs 4*C* and 5*C*) with an average increase of ∼2.5-fold for 8A-VFP/8C-mCh (Fig. 4*D*) and ∼2-fold for 8A-VFP/8D-mCh (Fig. 5*D*), suggesting that these channel subunits are slightly depressed by a constitutive baseline oxidation.

The inhibition of 8A-VFP/8C-mCh and 8A-VFP/8D-mCh channels by chloramine-T was pronounced even on hypotonically activated currents of these constructs (Fig. 6). Chloramine-T had no effect on basal currents in oocytes expressing WT 8A/8C or 8A/8D channels (data not shown). However, as seen for the fluorescently tagged constructs, chloramine-T strongly inhibited and DTT slightly increased hypotonically activated 8A/8C and 8A/8D WT channels (Fig. 7). However, due to the relatively small expression levels of untagged 8A/8C and 8A/8D channels, a quantitative evaluation of the effects is more difficult compared to the fluorescently tagged versions.

Expression of 8A/8B or 8A-VFP/8B-mCh subunits did not give rise to functional expression (Voss *et al.* 2014; Gaitán-Peñas *et al.* 2016). Unfortunately, neither the application of chloramine-T nor that of DTT on oocytes co-expressing fluorescently tagged 8A-VFP and 8B-mCh subunits elicited any currents above background (data not shown).

Chemical identity and localization of oxidized residues

An important question is whether the oxidation/reduction processes regulating LRRC8 channels are taking place in the intracellular or in the extracellular space. The delay in the onset of the effect of chloramine-T and TBHP suggests an intracellular action. To distinguish between these possibilities, and in addition, to identify the chemical identity of the residues involved, we employed various cysteine-modifying reagents. We first used the membrane-permeant cysteine reactive compound *S*-methyl methanethiosulfonate (MMTS). Application of MMTS to 8A-VFP/8E-mCh channels resulted in an approximate doubling of currents (Fig. 8*A* and *D*). More importantly, subsequent application of chloramine-T had practically no effect (Fig. 8*A* and *E*). This strongly suggests that the dramatic activation of 8A-VFP/8E-mCh by chloramine-T (Fig. 1) is mediated by the oxidation of cysteine residues, and that their oxidation by chloramine-T is prevented by prior modification by MMTS. To test the intracellular *vs.* extracellular location of the relevant cysteine residue(s), we applied charged MTS reagents. Application of the positively charged MTSET had no effect on 8A-VFP/8E-mCh mediated currents (Fig. 8*B* and *D*). Furthermore, treatment with MTSET slightly reduced, but did not prevent a strong activation of 8A-VFP/8E-mCh currents by chloramine-T

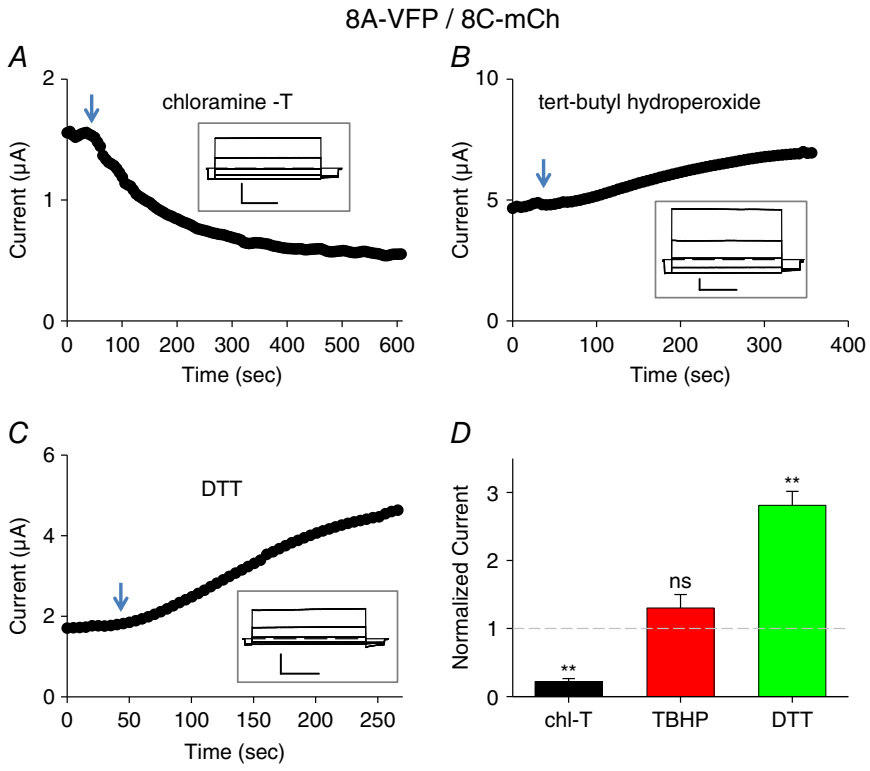

Figure 4. Effects of redox conditions on 8A-VFP/8C-mCh
A–C, typical experiments illustrating the effect of application of 1 mM chloramine-T (*A*), 1 mM TBHP (*B*) or 10 mM DTT (*C*) to oocytes co-expressing 8A-VFP and 8C-mCh at the indicated time points. The inset shows response to an *I–V* stimulation before stimulus application. Horizontal scale bars, 1 s; vertical scale bars, 1 μA. *D*, average response to the indicated stimuli, normalized to the initial current (one-sample *t* test with respect to control value 1, chl-T, $P = 3 \times 10^{-8}$**, $n = 10$; TBHN, $P = 0.24$, $n = 3$; DTT, $P = 0.0003$**, $n = 6$; error bars indicate SEM). Note the different time and current scales in the various panels. [Colour figure can be viewed at wileyonlinelibrary.com]

(Fig. 8*B* and *E*), suggesting that the relevant cysteine residue(s) are not located on the extracellular side. Interestingly, application of the negatively charged MTSES reagent, while not affecting currents of 8A-VFP/8E-mCh channels by itself (Fig. 8*C* and *D*), markedly reduced the activation of currents by the subsequent application of chloramine-T (Fig. 8*C*) to a 2-fold increase compared to the more than 10-fold increase without prior treatment (Fig. 8*C* and *E*). This result is compatible with the hypothesis that MTSES can enter the oocytes through the pore of 8A-VFP/8E-mCh channels and it is consistent with the permeability of these channels to relatively large organic molecules (Planells-Cases *et al.* 2015; Gaitán-Peñas *et al.* 2016; Gradogna *et al.* 2017; Lutter *et al.* 2017).

Similar to 8A-VFP/8E-mCh, application of cysteine-modifying reagents on 8A-VFP/8C-mCh channels had little direct effects (Fig. 9*A*). However, application of none of the cysteine-modifying reagents (MMTS, MTSET or MTSES) altered in a significant manner the subsequent effect of chloramine-T-induced reduction of currents (Fig. 9*B*). This result suggests that cysteine residues are not primarily involved in the oxidation-mediated current reduction of 8A-VFP/8C-mCh channels.

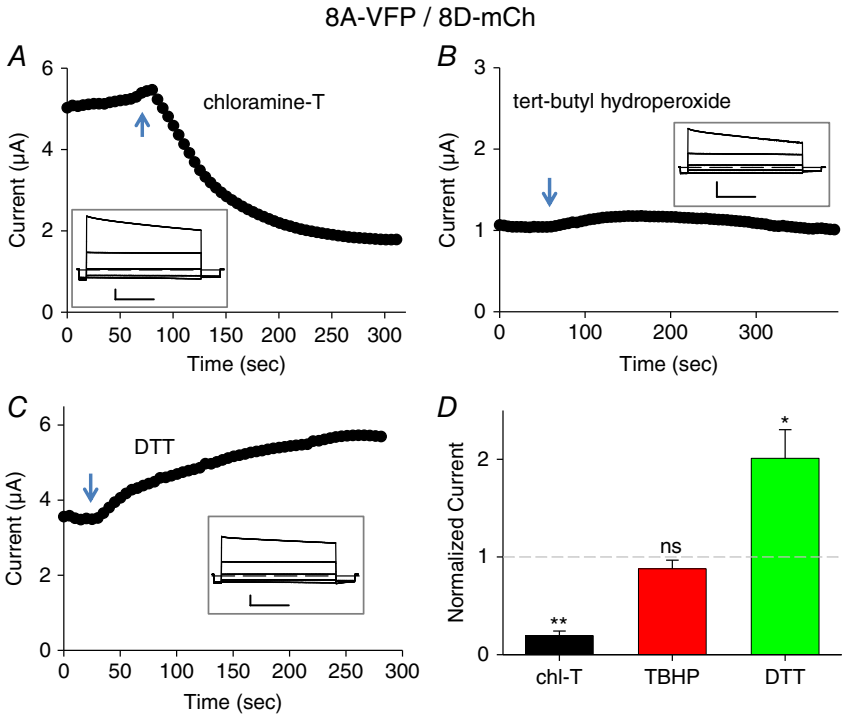

Figure 5. Effects of redox conditions on 8A-VFP/8D-mCh
A–*C*, typical experiments illustrating the effect of application of 1 mM chloramine-T (*A*), 1 mM TBHP (*B*) or 10 mM DTT (*C*) to oocytes co-expressing 8A-VFP and 8D-mCh at the indicated time points. The inset shows response to an *I*–*V* stimulation before stimulus application. Horizontal scale bars, 1 s; vertical scale bars, 1 μA (*A* and *C*) and 0.5 μA (*B*). *D*, average response to the indicated stimuli, normalized to the initial current (one-sample *t* test with respect to control value 1, chl-T, $P = 0.0004$**, $n = 4$; TBHN, $P = 0.26$, $n = 4$; DTT, $P = 0.041$*, $n = 4$; error bars indicate SEM). Note the different time and current scales in the various panels. [Colour figure can be viewed at wileyonlinelibrary.com]

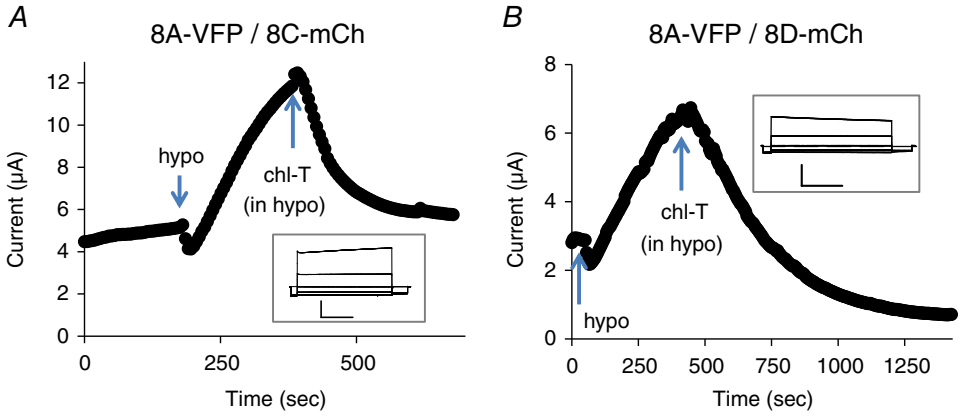

Figure 6. Effect of chloramine-T on hypotonicity-activated 8A-VFP/8C-mCh (*A*) and 8A-VFP/8D-mCh (*B*)
The insets show responses to an *I*–*V* stimulation before hypotonic stimulation. Horizontal scale bars, 1 s; vertical scale bars, 2 μA. Similar results were obtained for $n = 3$ oocytes each. Note the different time and current scales in the various panels. [Colour figure can be viewed at wileyonlinelibrary.com]

Effects of cysteine-modifying reagents on 8A-VFP/8D-mCh were more complex. For 8A-VFP/8D-mCh application of MMTS, MTSET and to a lesser degree also MTSES by themselves led to a significant current decrease with respect to basal level (Fig. 9*C*). Yet, subsequent application of chloramine-T induced a further reduction of currents as without prior cysteine modification (Fig. 9*D*). These results suggest an involvement of cysteine as well as other residues in the redox regulation of 8A-VFP/8D-mCh channels.

Oxidation-induced VRAC current decrease in the Jurkat T cell line

In order to test if the above-described effects of oxidative stress on VRAC channels may be of relevance *in vivo*, as a proof of principle, we concentrated on cells of the immune system. Oxidative stress plays an important role in the immune response in healthy (Belikov *et al.* 2015) and in tumour tissue (Chen *et al.* 2016). In addition, VRAC had been first identified (Cahalan & Lewis, 1988) and well studied in T lymphocytes (Nilius *et al.* 1997). A distinguishing feature of VRAC in lymphocytes and in the Jurkat T lymphocyte cell line is the absence of a significant time-dependent inactivation process at positive voltages (Lepple-Wienhues *et al.* 1998), consistent with the hypothesis that VRAC currents in T lymphocytes are mostly carried by LRRC8A–LRRC8C heteromers (Voss *et al.* 2014; Gaitán-Peñas *et al.* 2016; Ullrich *et al.* 2016). Thus, *a priori*, given our results on heterologously expressed LRRC8 proteins, oxidation, for example induced by the application of chloramine-T, is expected to decrease VRAC currents in T lymphocytes. To test this prediction, we used two different protocols to activate VRAC in the Jurkat T lymphocyte cell line. First, we employed a hypertonic pipette solution (~390 mosmol l^{-1}) which leads to the activation of VRAC about 1 min after establishing the whole-cell configuration (Fig. 10*A* and *B*). Currents showed the typical outward rectification and lack of inactivation as expected (Lepple-Wienhues *et al.* 1998; Fig. 10*A*, inset). Application of chloramine-T after significant current activation led to an almost immediate current inhibition in all cells tested (Fig. 10*A* and *B*; average inhibition: 59 ± 6%, $n = 8$). Very similar inhibition by chloramine-T was seen when currents were activated by a hypotonic extracellular solution (212 mosmol l^{-1}) (Fig. 10*C* and *D*; average inhibition: 57 ± 8%, $n = 5$). These results

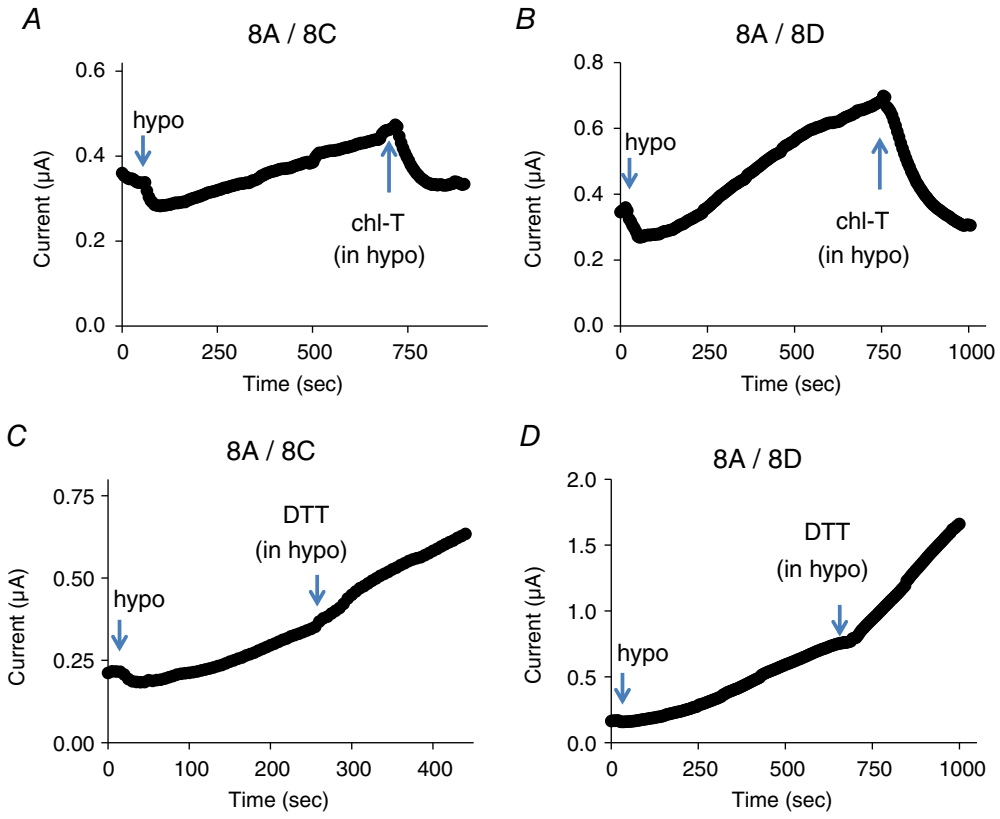

Figure 7. Effect of chloramine-T and DTT on hypotonicity-activated WT 8A/8C (*A* and *C*) and 8A/8D (*B* and *D*) channels
Similar results were obtained for $n \geq 3$ oocytes each. Note the different time and current scales in the various panels. [Colour figure can be viewed at wileyonlinelibrary.com]

suggest that VRAC currents in Jurkat cells are not carried in a significant manner by LRRC8A–LRRC8E heteromers.

Expression of LRRC8 genes Jurkat cells

We used real time PCR to evaluate the degree of expression of the various LRRC8 genes in Jurkat cells. Primer pairs were selected to produce fragments of 109–146 bp for all LRRC8 genes. Absolute quantification was performed by generating standard reference curves for all target genes (*LRRC8A–E*, see Methods for details) and determining the performance of the qPCR assay through estimation of the efficiency, which showed values ranging from 85 to 92%, rather similar for all cDNAs (Fig. 11*A*). RT-qPCR performed on retrotranscribed cDNA from Jurkat cell RNA indicated that transcriptional activity changes significantly among the different subunits with LRRC8D being the most expressed, followed by 8C and 8B, while LRRC8A and 8E were about one order of magnitude less expressed (Fig. 11*B*). Thus, in agreement with the results that oxidation by chloramine-T leads to a current reduction, the LRRC8E subunit is the least expressed in Jurkat cells.

Discussion

Oxidative processes play important roles in physiology and in pathological conditions as for example in cancer and ageing. Volume-regulated anion channels are ubiquitously expressed in practically all cell types and their activity has been linked directly or indirectly to ROS activity in many different physiological and pathophysiological contexts. ROS are generated by hypotonic cell swelling

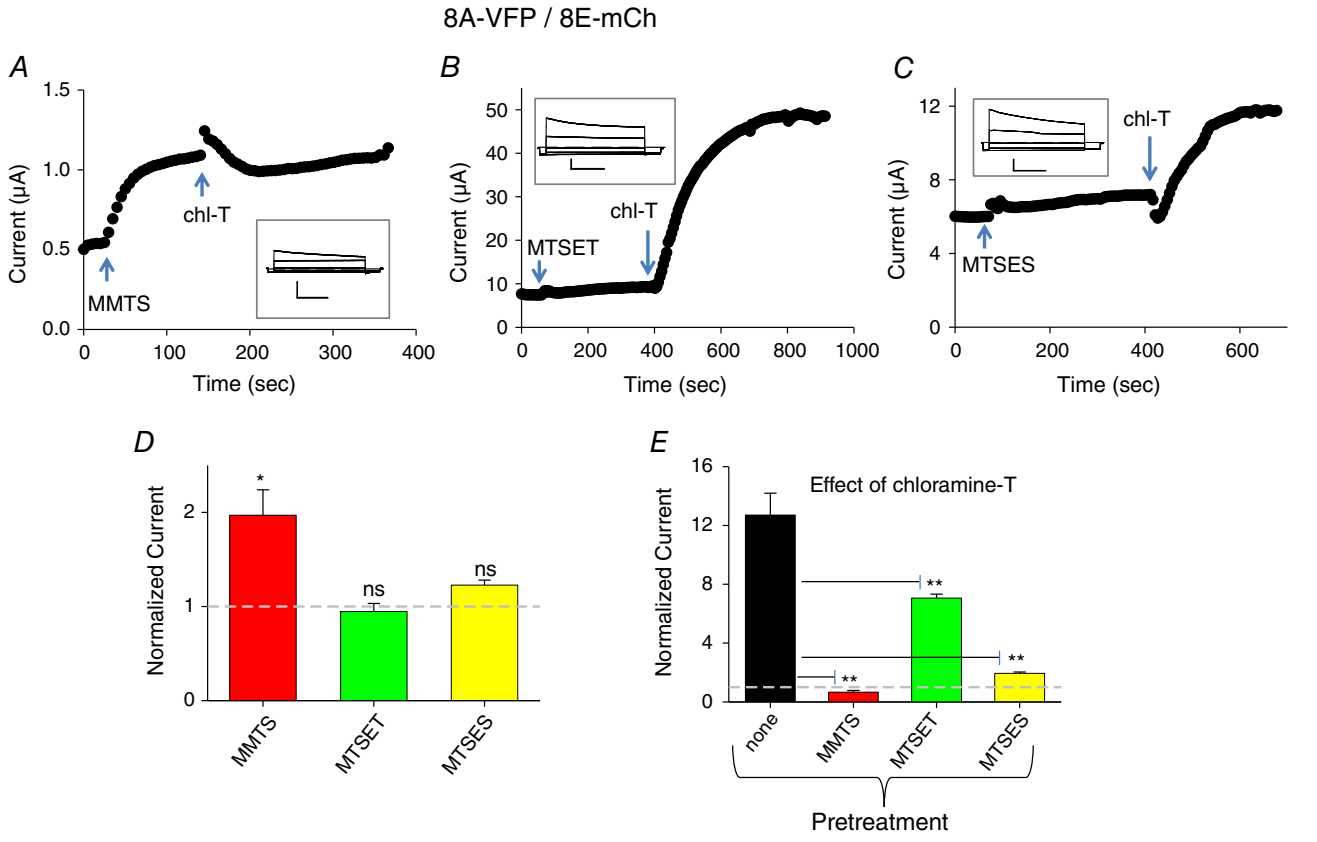

Figure 8. Effect of cysteine-modifying reagents on chloramine-T action on 8A-VFP/8E-mCh heteromers
A–C, typical experiments illustrating the effect of application of 1 mM MMTS (*A*), MTSET (*B*), and MTSES (*C*) and subsequent application of 1 mM chloramine-T on different 8A-VFP/8E-mCh-expressing oocytes. The insets show traces before application of the cysteine-reactive compounds. Horizontal scale bars, 1 s; vertical scale bars, 0.5 μA (*A*) and 2 μA (*B* and *C*). *D*, effect of cysteine-modifying reagents, normalized to the basal current (indicated by a dashed line; one-sample *t* test with respect to control value 1, MMTS, $P = 0.037$*, $n = 4$; MTSET, $P = 0.59$, $n = 3$; MTSES, $P = 0.052$, $n = 3$; error bars indicate SEM). *E*, average response to the application of 1 mM chloramine-T after pretreatment with cysteine-modifying reagents, normalized to the current before chloramine-T application ($n \geq 3$ each, error bars indicate SEM). The column indicated by 'none' is the same as that of Fig. 1*D*. Pretreatment with cysteine-modifying reagents decreased in a significant manner the subsequent effect of chloramine-T (ANOVA, *post hoc* Tukey's test, $P < 0.01$** indicated only with respect to no pretreatment). Note the different time and current scales in the various panels. [Colour figure can be viewed at wileyonlinelibrary.com]

in various cell types (Lambert, 2003; Crutzen *et al.* 2012; Holm *et al.* 2013), and in concert, in several cell types ROS appear to activate VRAC currents (Shimizu *et al.* 2004; Varela *et al.* 2004, 2007; Wang *et al.* 2005, 2017*a*, *b*; Harrigan *et al.* 2008; Liu *et al.* 2009; Deng *et al.* 2010; Crutzen *et al.* 2012; Holm *et al.* 2013; Shen *et al.* 2014; Xia *et al.* 2016).

However, a critical open question regarding the role of ROS in processes involving VRAC is whether oxidation directly acts on the channel forming proteins (i.e. LRRC8 proteins) or if ROS act on other cellular components involved in VRAC modulation. This question is extremely difficult to address in a cellular system because in order to monitor VRAC function, the channels have first to be activated, for example by extracellular hypotonicity. However, the activation mechanism is poorly understood, but is known to involve factors like protein kinases (Nilius *et al.* 1997; Jentsch, 2016; Pedersen *et al.* 2016). Thus, it is difficult to determine whether oxidation acts on such factors or directly on the channel protein. Here we took advantage of the recent finding that LRRC8 subunits that are C-terminally tagged with fluorescent proteins give rise to constitutive currents in *Xenopus* oocytes (Gaitán-Peñas *et al.* 2016). This allowed us to study direct effects of oxidizing and reducing agents on LRRC8-mediated VRAC channel activity.

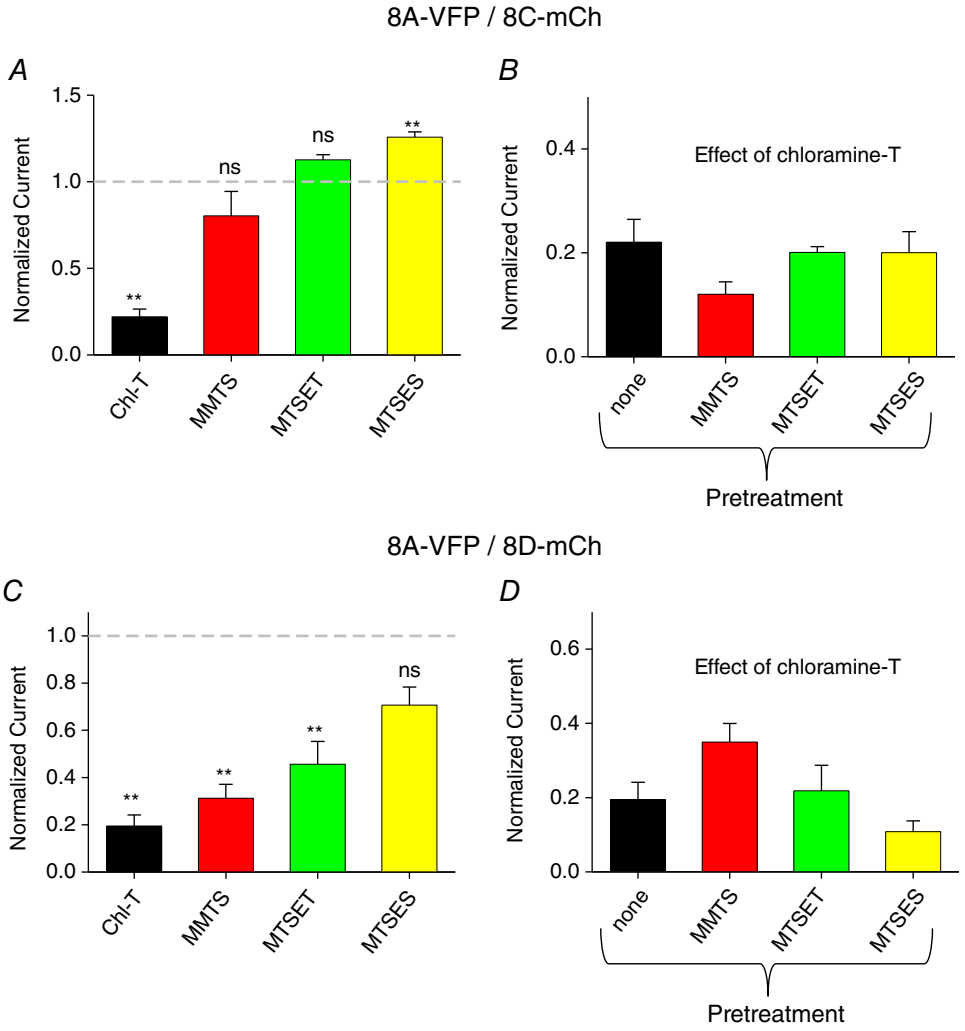

Figure 9. Effect of cysteine modifying reagents on 8A-VFP/8C-mCh and 8A-VFP/8D-mCh heteromers
A and *C*, effect of cysteine-modifying reagents on 8A-VFP/8C-mCh (*A*) and 8A-VFP/8D-mCh (*C*) co-expressing oocytes. One-sample *t* test with respect to control value 1. In *A*, Chl-T, $P = 3 \times 10^{-8}$** as in Fig. 4; MMTS, $P = 0.25$, $n = 4$; MTSET, $P = 0.050$, $n = 3$; MTSES, $P = 0.004$**, $n = 3$. In *C*, Chl-T, $P = 0.0004$** as in Fig. 5; MMTS, $P = 0.0013$**, $n = 4$; MTSET, $P = 0.03$*, $n = 3$; MTSES, $P = 0.06$, $n = 3$. *B* and *D*, effect of subsequent application of chloramine-T in the presence of cysteine-modifying agents in the bath. No significant alteration of chloramine-T-induced reduction of currents was observed (ANOVA: $P = 0.34$ (*B*); $P = 0.23$ (*D*); $n \geq 3$ each, error bars indicate SEM). Note the different time and current scales in the various panels. [Colour figure can be viewed at wileyonlinelibrary.com]

Surprisingly, we found that channels composed of different subunit combinations responded in opposite manners to oxidation. 8A-VFP/8E-mCh channels were dramatically potentiated by oxidation with chloramine-T as well as by TBHP, whereas 8A-VFP/8C-mCh and 8A-VFP/8D-mCh channels were markedly inhibited by chloramine-T oxidation. Conversely, whereas 8A-VFP/8E-mCh channels were unaffected by DTT, 8A-VFP/8C-mCh and 8A-VFP/8D-mCh channels were significantly augmented by DTT, suggesting a constitutive oxidative inhibition of these channels. Somewhat surprisingly, 8A-VFP/8C-mCh channels were slightly activated by TBHP and 8A-VFP/8D-mCh were unaffected by TBHP. Thus, either the relevant residues in 8A-VFP/8C-mCh and 8A-VFP/8D-mCh channels, whose oxidation by chloramine-T leads to channel inactivation, are not modified by TBHP or their oxidation by TBHP is of a different chemical character. Similar different sensitivity to chloramine-T *versus* TBHP has also been observed in two-pore domain potassium channels (Duprat *et al.* 2005).

Such a differential effect of chloramine-T and the differential effect on the various heteromers strongly suggest that the relevant oxidation reactions directly affect the channel protein and not other molecules involved in volume activation. Otherwise, a parallel effect would have to be expected for all subunit combinations, as all heteromers are activated by hypotonic stimulation. However, our experiments do not provide a direct biochemical proof that the effects are mediated by an oxidation of the LRRC8 proteins.

A further important conclusion that can be drawn from our experiments is that oxidation of 8A-VFP/8E-mCh is not a necessary event for volume stimulation of the channels, but rather modulates channel open probability in addition to the activation by a hypotonic stimulation. In fact, oxidation of 8A-VFP/8E-mCh and also of WT 8A/8E channels after volume stimulation further enhances the currents (Fig. 3). This result is also in agreement with the hypothesis that the direct physico-chemical signal mediating VRAC activation is low intracellular ionic strength (Nilius *et al.* 1998; Syeda *et al.* 2016).

Several lines of evidence support the conclusion that the oxidative potentiation of 8A/8E channels involves intracellularly accessible cysteine residue(s). First, effects of chloramine-T and TBHP occurred with a significant delay, suggesting that the compounds had to enter the oocytes. Secondly, effects were completely blocked by the membrane permeable cysteine-modifying MMTS reagent, but not by the positively charged MTSET reagent. Interestingly, the negatively charged MTSES partially inhibited subsequent activation by chloramine-T. This is consistent with the hypothesis that MTSES can permeate the channel and exert its effect from the inside or that cysteine residues located in the pore could be involved. The permeation of such a large organic molecule is in agreement with the permeability of 8A/8E for several amino acids, taurine, *myo*-inositol, cisplatin and even ATP (Voss *et al.* 2014;

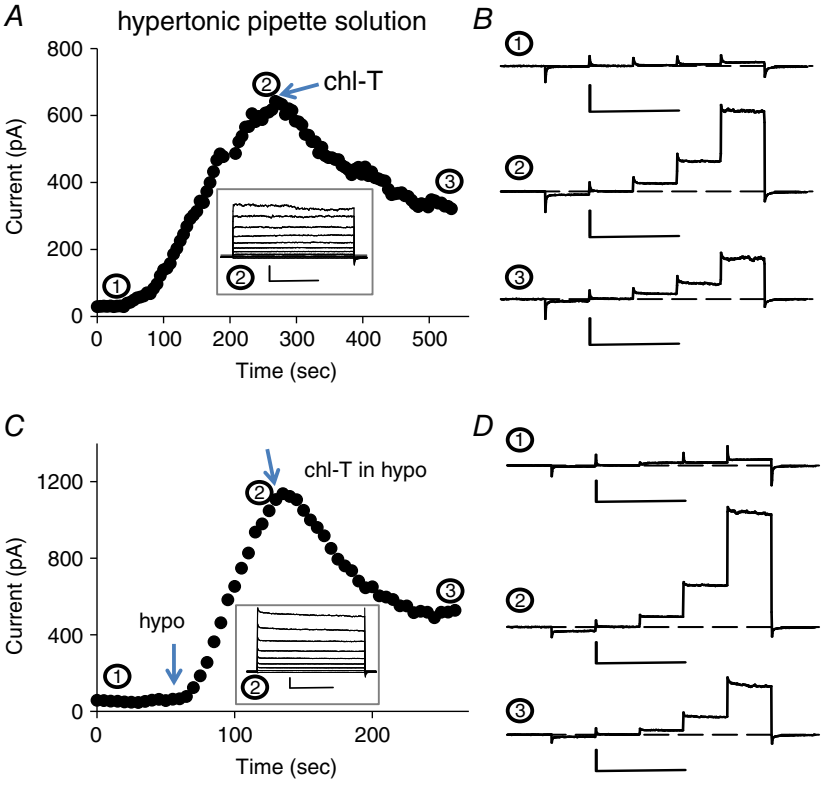

Figure 10. Effect of chloramine-T on volume-dependent anion currents in Jurkat T cells
A and *B*, typical experiment illustrating the effect of application of 500 μM chloramine-T on a cell after stimulation of VRAC by a hypertonic intracellular solution. The current at 100 mV is plotted as a function of time. The traces in *B* show the current response to 50 ms steps to −100, −50, 0, 50 and 100 mV at the indicated time points (horizontal scale bars, 100 ms; vertical scale bars, 200 pA). *C* and *D*, typical experiment illustrating the effect of application of 500 μM chloramine-T on a cell after stimulation of VRAC by a hypotonic extracellular solution. Insets show the response to an *I–V* stimulation after maximal activation. Horizontal scale bars, 200 ms; vertical scale bars, 200 pA. [Colour figure can be viewed at wileyonlinelibrary.com]

Gaitán-Peñas *et al.* 2016; Gradogna *et al.* 2017; Lutter *et al.* 2017).

In contrast, the oxidation-induced inhibition of 8A/8C channels is likely not mediated by cysteine residues because pretreatment with MMTS, MTSES or MTSET did not prevent subsequent chloramine-T-induced inhibition. It can be speculated that for example methionine residues are involved in the inhibition.

The situation is less clear for 8A/8D because MMTS, while inhibiting the channels by itself, only slightly impeded subsequent inhibition by chloramine-T. This suggests the involvement of cysteine as well as non-cysteine residues in redox regulation of this subunit combination.

The fact that endogenous LRRC8 channels are most likely heteromers of variable stoichiometry that contain more than two different LRRC8 subunits (Gaitán-Peñas *et al.* 2016; Lutter *et al.* 2017) renders the redox regulation of VRAC channels extremely complex. Here, we tested effects of oxidation on endogenous VRAC currents in Jurkat T lymphocytes. In general, ROS play an extremely important role in the immune system both for direct killing activity, for example by phagocytic leukocytes, and as second messengers for T cell activation (Belikov *et al.* 2015). VRAC has been well studied in T lymphocytes, the cells where a volume-regulated anion current actually had been described for the first time (Cahalan & Lewis, 1988). In a single heterozygous patient, a truncation of the two terminal leucine-rich repeats was reported to be associated with agammaglobulinaemia and the absence of circulating B cells (Sawada *et al.* 2003). Furthermore, complete knockout of LRRC8A led to a severe defect in T and B cell development (Kumar *et al.* 2014). However, surprisingly, truncation of the terminal 15 leucine-rich repeats of LRRC8A in the *ebo* mouse line did not impair T cell development nor change T cell function, even though VRAC channel activity was practically absent in T cells from these mice (Platt *et al.* 2017). Thus, the physiological role of VRAC in T cells is still unclear.

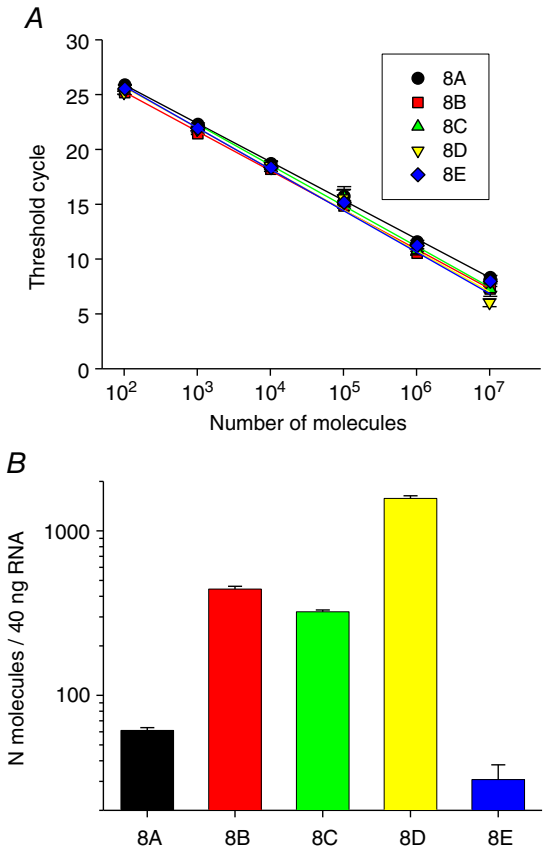

Figure 11. Quantification of LRRC8 subunit expression in Jurkat cells
A, standard curves of *LRRC8A–E* are shown. Curves were generated performing qPCR on serial dilutions of the plasmids containing the respective cDNAs. The lines represent the best linear fit to the experimental data. Error bars indicate standard deviation. Slope, *y*-intercept of the linear fit and calculated efficiency are, respectively: 8A: −3.53, 32.9, 92%; 8B: −3.59, 32.4, 89.9%; 8C: −3.71, 33.4, 85.9%; 8D: −3.78; 33.2, 84.6%; 8E: −3.52, 32.5; 92.5%. *B*, expression of LRRC8 subunits reported as number of molecules in 40 ng of RNA, as determined from the calibration curve shown in *A*. Data are from two independent experiments and six technical replicates. [Colour figure can be viewed at wileyonlinelibrary.com]

A peculiar feature of VRAC in T cells is the almost complete lack of inactivation at positive voltages (Lepple-Wienhues *et al.* 1998). Among all binary LRRC8 combinations, 8A/8C channels exhibit the least degree of inactivation (Voss *et al.* 2014; Gaitán-Peñas *et al.* 2016; Ullrich *et al.* 2016), suggesting that the endogenous VRAC currents in T cells are carried in a significant manner by 8A/8C channels. In agreement with this hypothesis, we found that VRAC currents are significantly suppressed by oxidation in Jurkat cells. Furthermore, we found that the 8E subunit, which would be expected to confer an activating effect of oxidation, is the least expressed in Jurkat cells. We found the 8D subunit to be the one of highest expression in Jurkat cells. *A priori*, 8D-containing channels might be expected to exhibit an inactivating current phenotype (Voss *et al.* 2014; Gaitán-Peñas *et al.* 2016). However, the biophysical properties of channels composed of more than two different LRRC8 subunits are unknown.

In summary, we found that VRAC channels composed of LRRC8 proteins are directly modulated by oxidation, with 8A/8E heteromers being dramatically activated by the oxidation of intracellular cysteines, whereas 8A/8C and 8A/8D heteromers are drastically inhibited. In agreement with the non-inactivating current characteristic of VRAC in T lymphocytes that is a typical feature of the 8C subunit, we found that VRAC currents in Jurkat cells are inhibited by oxidation and that the 8E subunit is the least expressed in Jurkat cells. We speculate that a reduction of VRAC during acute T cell activation associated with ROS production might be of physiological relevance in the immune response.

References

Abascal F & Zardoya R (2012). LRRC8 proteins share a common ancestor with pannexins, and may form hexameric channels involved in cell-cell communication. *Bioessays* **34**, 551–560.

Behe P, Foote JR, Levine AP, Platt CD, Chou J, Benavides F, Geha RS & Segal AW (2017). The LRRC8A mediated "swell activated" chloride conductance is dispensable for vacuolar homeostasis in neutrophils. *Front Pharmacol* **8**, 262.

Belikov AV, Schraven B & Simeoni L (2015). T cells and reactive oxygen species. *J Biomed Sci* **22**, 85.

Browe DM & Baumgarten CM (2004). Angiotensin II (AT1) receptors and NADPH oxidase regulate Cl^- current elicited by β1 integrin stretch in rabbit ventricular myocytes. *J Gen Physiol* **124**, 273–287.

Cahalan MD & Lewis RS (1988). Role of potassium and chloride channels in volume regulation by T lymphocytes. *Soc Gen Physiol Ser* **43**, 281–301.

Chen X, Song M, Zhang B & Zhang Y (2016). Reactive oxygen species regulate T cell immune response in the tumor microenvironment. *Oxid Med Cell Longev* **2016**, 1580967.

Crutzen R, Shlyonsky V, Louchami K, Virreira M, Hupkens E, Boom A, Sener A, Malaisse WJ & Beauwens R (2012). Does NAD(P)H oxidase-derived H_2O_2 participate in hypotonicity-induced insulin release by activating VRAC in β-cells? *Pflugers Arch* **463**, 377–390.

DeCoursey TE (2003). Voltage-gated proton channels and other proton transfer pathways. *Physiol Rev* **83**, 475–579.

Deng W, Baki L, Yin J, Zhou H & Baumgarten CM (2010). HIV protease inhibitors elicit volume-sensitive Cl^- current in cardiac myocytes via mitochondrial ROS. *J Mol Cell Cardiol* **49**, 746–752.

Duprat F, Girard C, Jarretou G & Lazdunski M (2005). Pancreatic two P domain K^+ channels TALK-1 and TALK-2 are activated by nitric oxide and reactive oxygen species. *J Physiol* **562**, 235–244.

Gaitán-Peñas H, Gradogna A, Laparra-Cuervo L, Solsona C, Fernández-Dueñas V, Barrallo-Gimeno A, Ciruela F, Lakadamyali M, Pusch M & Estévez R (2016). Investigation of LRRC8-mediated volume-regulated anion currents in *Xenopus* oocytes. *Biophys J* **111**, 1429–1443.

Gradogna A, Gaitan-Penas H, Boccaccio A, Estevez R & Pusch M (2017). Cisplatin activates volume sensitive LRRC8 channel mediated currents in *Xenopus* oocytes. *Channels (Austin)* **11**, 254–260.

Harrigan TJ, Abdullaev IF, Jourd'heuil D & Mongin AA (2008). Activation of microglia with zymosan promotes excitatory amino acid release via volume-regulated anion channels: the role of NADPH oxidases. *J Neurochem* **106**, 2449–2462.

Holm JB, Grygorczyk R & Lambert IH (2013). Volume-sensitive release of organic osmolytes in the human lung epithelial cell line A549: role of the 5-lipoxygenase. *Am J Physiol Cell Physiol* **305**, C48–C60.

Jentsch TJ (2016). VRACs and other ion channels and transporters in the regulation of cell volume and beyond. *Nat Rev Mol Cell Biol* **17**, 293–307.

Kumar L, Chou J, Yee CS, Borzutzky A, Vollmann EH, von Andrian UH, Park SY, Hollander G, Manis JP, Poliani PL & Geha RS (2014). Leucine-rich repeat containing 8A (LRRC8A) is essential for T lymphocyte development and function. *J Exp Med* **211**, 929–942.

Lambert IH (2003). Reactive oxygen species regulate swelling-induced taurine efflux in NIH3T3 mouse fibroblasts. *J Membr Biol* **192**, 19–32.

Le Gal K, Ibrahim MX, Wiel C, Sayin VI, Akula MK, Karlsson C, Dalin MG, Akyurek LM, Lindahl P, Nilsson J & Bergo MO (2015). Antioxidants can increase melanoma metastasis in mice. *Sci Transl Med* **7**, 308re308.

Lepple-Wienhues A, Szabo I, Laun T, Kaba NK, Gulbins E & Lang F (1998). The tyrosine kinase p56lck mediates activation of swelling-induced chloride channels in lymphocytes. *J Cell Biol* **141**, 281–286.

Lewis RS, Ross PE & Cahalan MD (1993). Chloride channels activated by osmotic stress in T lymphocytes. *J Gen Physiol* **101**, 801–826.

Liu HT, Akita T, Shimizu T, Sabirov RZ & Okada Y (2009). Bradykinin-induced astrocyte-neuron signalling: glutamate release is mediated by ROS-activated volume-sensitive outwardly rectifying anion channels. *J Physiol* **587**, 2197–2209.

Lopez-Otin C, Blasco MA, Partridge L, Serrano M & Kroemer G (2013). The hallmarks of aging. *Cell* **153**, 1194–1217.

Lutter D, Ullrich F, Lueck JC, Kempa S & Jentsch TJ (2017). Selective transport of neurotransmitters and modulators by distinct volume-regulated LRRC8 anion channels. *J Cell Sci* **130**, 1122–1133.

Muralidharan S & Mandrekar P (2013). Cellular stress response and innate immune signaling: integrating pathways in host defense and inflammation. *J Leukoc Biol* **94**, 1167–1184.

Nilius B, Eggermont J, Voets T, Buyse G, Manolopoulos V & Droogmans G (1997). Properties of volume-regulated anion channels in mammalian cells. *Prog Biophys Mol Biol* **68**, 69–119.

Nilius B, Prenen J, Voets T, Eggermont J & Droogmans G (1998). Activation of volume-regulated chloride currents by reduction of intracellular ionic strength in bovine endothelial cells. *J Physiol* **506**, 353–361.

Okada Y, Sato K & Numata T (2009). Pathophysiology and puzzles of the volume-sensitive outwardly rectifying anion channel. *J Physiol* **587**, 2141–2149.

Pedersen SF, Okada Y & Nilius B (2016). Biophysics and physiology of the volume-regulated anion channel (VRAC)/volume-sensitive outwardly rectifying anion channel (VSOR). *Pflugers Arch* **468**, 371–383.

Piskounova E, Agathocleous M, Murphy MM, Hu Z, Huddlestun SE, Zhao Z, Leitch AM, Johnson TM, DeBerardinis RJ & Morrison SJ (2015). Oxidative stress inhibits distant metastasis by human melanoma cells. *Nature* **527**, 186–191.

Planells-Cases R, Lutter D, Guyader C, Gerhards NM, Ullrich F, Elger DA, Kucukosmanoglu A, Xu G, Voss FK, Reincke SM, Stauber T, Blomen VA, Vis DJ, Wessels LF, Brummelkamp TR, Borst P, Rottenberg S & Jentsch TJ (2015). Subunit composition of VRAC channels determines substrate specificity and cellular resistance to Pt-based anti-cancer drugs. *EMBO J* **34**, 2993–3008.

Platt CD, Chou J, Houlihan P, Badran YR, Kumar L, Bainter W, Poliani PL, Perez CJ, Dent SY, Clapham DE, Benavides F & Geha RS (2017). Leucine-rich repeat containing 8A (LRRC8A)-dependent volume-regulated anion channel activity is dispensable for T-cell development and function. *J Allergy Clin Immunol* (in press; https://doi.org/10.1016/j.jaci.2016.12.974).

Qiu Z, Dubin AE, Mathur J, Tu B, Reddy K, Miraglia LJ, Reinhardt J, Orth AP & Patapoutian A (2014). SWELL1, a plasma membrane protein, is an essential component of volume-regulated anion channel. *Cell* **157**, 447–458.

Sawada A, Takihara Y, Kim JY, Matsuda-Hashii Y, Tokimasa S, Fujisaki H, Kubota K, Endo H, Onodera T, Ohta H, Ozono K & Hara J (2003). A congenital mutation of the novel gene LRRC8 causes agammaglobulinemia in humans. *J Clin Invest* **112**, 1707–1713.

Schwab A, Fabian A, Hanley PJ & Stock C (2012). Role of ion channels and transporters in cell migration. *Physiol Rev* **92**, 1865–1913.

Shen M, Wang L, Wang B, Wang T, Yang G, Shen L, Guo X, Liu Y, Xia Y, Jia L & Wang X (2014). Activation of volume-sensitive outwardly rectifying chloride channel by ROS contributes to ER stress and cardiac contractile dysfunction: involvement of CHOP through Wnt. *Cell Death Dis* **5**, e1528.

Shimizu T, Numata T & Okada Y (2004). A role of reactive oxygen species in apoptotic activation of volume-sensitive Cl^- channel. *Proc Natl Acad Sci U S A* **101**, 6770–6773.

Syeda R, Qiu Z, Dubin AE, Murthy SE, Florendo MN, Mason DE, Mathur J, Cahalan SM, Peters EC, Montal M & Patapoutian A (2016). LRRC8 Proteins form volume-regulated anion channels that sense ionic strength. *Cell* **164**, 499–511.

Ullrich F, Reincke SM, Voss FK, Stauber T & Jentsch TJ (2016). Inactivation and anion selectivity of volume-regulated anion channels (VRACs) depend on C-terminal residues of the first extracellular loop. *J Biol Chem* **291**, 17040–17048.

Varela D, Simon F, Olivero P, Armisen R, Leiva-Salcedo E, Jorgensen F, Sala F & Stutzin A (2007). Activation of H_2O_2-induced VSOR Cl^- currents in HTC cells require phospholipase Cγ1 phosphorylation and Ca^{2+} mobilisation. *Cell Physiol Biochem* **20**, 773–780.

Varela D, Simon F, Riveros A, Jorgensen F & Stutzin A (2004). NAD(P)H oxidase-derived H_2O_2 signals chloride channel activation in cell volume regulation and cell proliferation. *J Biol Chem* **279**, 13301–13304.

Voss FK, Ullrich F, Munch J, Lazarow K, Lutter D, Mah N, Andrade-Navarro MA, von Kries JP, Stauber T & Jentsch TJ (2014). Identification of LRRC8 heteromers as an essential component of the volume-regulated anion channel VRAC. *Science* **344**, 634–638.

Wang L, Shen M, Guo X, Wang B, Xia Y, Wang N, Zhang Q, Jia L & Wang X (2017*a*). Volume-sensitive outwardly rectifying chloride channel blockers protect against high glucose-induced apoptosis of cardiomyocytes via autophagy activation. *Sci Rep* **7**, 44265.

Wang R, Lu Y, Gunasekar S, Zhang Y, Benson CJ, Chapleau MW, Sah R & Abboud FM (2017*b*). The volume-regulated anion channel (LRRC8) in nodose neurons is sensitive to acidic pH. *JCI Insight* **2**, e90632.

Wang X, Takahashi N, Uramoto H & Okada Y (2005). Chloride channel inhibition prevents ROS-dependent apoptosis induced by ischemia-reperfusion in mouse cardiomyocytes. *Cell Physiol Biochem* **16**, 147–154.

Xia Y, Liu Y, Xia T, Li X, Huo C, Jia X, Wang L, Xu R, Wang N, Zhang M, Li H & Wang X (2016). Activation of volume-sensitive Cl^- channel mediates autophagy-related cell death in myocardial ischaemia/reperfusion injury. *Oncotarget* **7**, 39345–39362.

Additional information

Competing interest

The authors declare no competing financial interests.

Author contributions

All authors contributed to the design of experiments, performed experiments, and analysed data. M.P. wrote the manuscript with input from all authors. All authors have approved the final version of the manuscript and agree to be accountable for all aspects of the work. All persons designated as authors qualify for authorship, and all those who qualify for authorship are listed.

Funding

The study was supported by a grant from the Fondazione Compagnia di San Paolo, Torino (2013.0922 to A.B.).

Acknowledgements

We thank Dr Raul Estévez for all plasmids and Francesa Quartino for excellent technical assistance.